Physics and Imaging in Radiation Oncology 20 (2021) 40–45

Contents lists available at ScienceDirect

Physics and Imaging in Radiation Oncology

journal homepage: www.sciencedirect.com/journal/physics-and-imaging-in-radiation-oncology

Characterisation of a synthetic diamond detector for end-to-end dosimetry in stereotactic body radiotherapy and radiosurgery

Maddison Shaw [a,b,*], Jessica Lye [a,c], Andrew Alves [a], Stephanie Keehan [a], Joerg Lehmann [d,e,f,g], Maximilian Hanlon [a], John Kenny [h], John Baines [i], Claudiu Porumb [j], Moshi Geso [b], Rhonda Brown [a]

[a] Australian Clinical Dosimetry Service, Australian Radiation Protection and Nuclear Safety Agency, Yallambie, VIC, Australia
[b] School of Health and Biomedical Science, RMIT University, Melbourne, VIC, Australia
[c] Olivia Newtown John Cancer Wellness & Research Centre, Heidelberg, VIC, Australia
[d] Department of Radiation Oncology, Calvary Mater Newcastle, Newcastle, Australia
[e] School of Science, RMIT University, Melbourne, Australia
[f] School of Mathematical and Physical Sciences, University of Newcastle, Australia
[g] Institute of Medical Physics, University of Sydney, Australia
[h] Medical Physics Specialists, Health Stem Solutions, Melbourne, VIC, Australia
[i] Radiation Oncology, Townsville Cancer Centre, Townsville, QLD, Australia
[j] Alfred Health Radiation Oncology, Melbourne VIC, Australia

ARTICLE INFO

Keywords:
microDiamond
SBRT
SRS
Dosimetry audit
Quality assurance
Small field dosimetry

ABSTRACT

Background and purpose: Synthetic diamond detectors offer real time measurement of dose in radiotherapy applications which require high spatial resolution. Additional considerations and corrections are required for measurements where the diamond detector is orientated at various angles to the incident beam. This study investigated diamond detectors for end-to-end testing of Stereotactic Body Radiotherapy (SBRT) and Stereotactic Radiosurgery (SRS) in the context of dosimetry audits.

Material and methods: Seven individual diamond detectors were investigated and compared with respect to warm up stability, dose-rate dependence, linearity, detector shadowing, energy response, cross-calibration, angular dependence and positional sensitivity in SBRT and SRS.

Results: Large variation in the cross calibration factors was found between the seven individual detectors. For each detector, the energy dependence in the cross calibration factor was on average <0.6% across the beam qualities investigated (Co-60 Gamma Knife, and MV beams with $TPR_{20,10}$ 0.684–0.733). The angular corrections for individual fields were up to 5%, and varied with field size. However, the average angular dependence for all fields in a typical SRS treatment delivery was <1%. The overall measurement uncertainty was 3.6% and 3.1% (2σ) for an SRS and SBRT treatment plan respectively.

Conclusion: Synthetic diamond detectors were found to be reliable and robust for end-to-end dosimetry in SBRT and SRS applications. Orientation of the detector relative to the beam axis is an important consideration, as significant corrections are required for angular dependence.

1. Introduction

Treatment techniques involving very small fields and enhanced treatment verification imaging, have enabled Stereotactic Radiosurgery (SRS) and Stereotactic Body Radiotherapy (SBRT) [1–3]. SRS and SBRT plans are characterised by high dose per fraction and steep dose gradients (~10%/mm), often in very close proximity to critical structures. Such techniques require high accuracy treatment delivery, in both congruence between calculated and delivered dose and in positional accuracy. Patient specific quality assurance (PSQA), involving verification of plans prior to patient treatment [4–7], and end-to-end testing in SRS and SBRT typically involve the use of a 2D detector, for assessment of spatial and dosimetric accuracy. Film, ion chamber arrays and diode arrays are popular detectors used for PSQA [8]. However array devices

* Corresponding author at: Australian Clinical Dosimetry Service, Australian Radiation Protection and Nuclear Safety Agency, Yallambie, VIC, Australia.
E-mail address: maddison.shaw@arpansa.gov.au (M. Shaw).

https://doi.org/10.1016/j.phro.2021.10.002
Received 21 April 2021; Received in revised form 9 October 2021; Accepted 10 October 2021

may lack the required spatial resolution for small field SRS and SBRT measurements [9]. Radiochromic film is often considered an ideal detector for SRS and SBRT QA due to the high spatial resolution [8,10,11], however significant post processing is required which is both labour and time intensive. Complementary point dose detector measurements enable real time analysis and provide a dosimetric comparison with the 2D detector. AAPM/IAEA TRS-483 recommends a number of point dose detectors for small field dosimetry [12].

Synthetic diamond detectors are favourable for radiotherapy applications requiring high spatial resolution due to their near water equivalence and small corrections factors compared to most other small field detectors [12]. Previous reports in the literature focus on the use of the diamond detectors for relative small field dosimetry, such as output factors and water tank scanning, where the detector axis is orientated parallel to the incident radiation beam [12–17]. Parallel orientation is recommended by TRS-483 due to the asymmetries in detector construction and potential for stem irradiation effects [12]. For PSQA and end-to-end testing, tissue equivalent QA phantoms often require detectors to be orientated perpendicular to beam delivery. For SRS and SBRT this concept is extended, as the treatment delivery may involve non-coplanar couch and gantry angles. Angular dependence of the diamond detectors in a perpendicular orientation has been investigated, however angular correction factors have not been presented [18]. In addition, direct dose measurements are not typically reported.

This work presents comprehensive characterisation of a synthetic diamond detector as an end-to-end dosimeter in SRS and SBRT QA, in the context of dosimetry audits. Seven individual diamond detectors were compared for a range of dosimetric properties, the first study to evaluate a considerable number of detectors.

2. Materials and methods

The Australian Clinical Dosimetry Service (ACDS) [19] performed on-site, end-to-end dosimetry audits of SRS and SBRT, in a cranial phantom (MAX-HD, Integrated Medical Technologies, Troy, NY, USA) and a thorax phantom (CIRS Inc., Norfolk, VA, USA), respectively. In both SRS and SBRT audits, Gafchromic EBT3 film (Ashland, Bridgwater, NJ, USA) was used as the primary detector for assessment of both positional and dosimetric accuracy of treatment delivery. Diamond detectors were used in both audits for real time measurements in target volumes $\geq$1.5 cm^3.

The PTW 60019 microDiamond detector (PTW Freiburg, Germany) is a synthetic diamond detector operated at zero bias voltage. It has a sensitive volume circular disk of 2 mm diameter and 2 μm thickness, with the effective point of measurement 1 mm from the detector end-face, on the detector axis. As recommended by TRS-483 [12], the microDiamond detector was orientated parallel to the beam axis for measurements such as output factors (Fig. 1a). In the ACDS end-to-end dosimetry audits, the detector was placed into anthropomorphic cranial (Fig. 1b) and thorax (Fig. 1c) phantoms, with the detector orientated craniocaudally (along the superior/inferior axis) in the phantoms. For a standard coplanar Linear Accelerator delivery, this orientation was considered perpendicular to the beam axis. Non-coplanar treatment deliveries, typical of SRS plans, were further explored in the context of angular dependence.

Seven microDiamond detectors were investigated for basic dosimetric properties, cross-calibration, positional sensitivity in SRS/SBRT, and angular dependence. All properties were evaluated for their contributing uncertainty leading to an overall assessment of measurement accuracy for the microDiamond in end-to-end testing of stereotactic fields. The measurements were performed on Elekta Versa HD and Synergy Linear Accelerators (Elekta AB, Stockholm, Sweden) located at the Australian Radiation Protection and Nuclear Safety Agency (ARPANSA, Melbourne, Australia).

2.1. Basic dosimetric properties

Two microDiamond detectors were sequentially setup in a full scatter water phantom (Blue Phantom^2, IBA dosimetry GmbH, Schwarzenbruck, Germany) at 90 cm source to surface distance (SSD), 10 cm depth, orientated perpendicular to the down-facing beam. Fields of 3x3 cm^2 were delivered to each detector with 6 MV, 6 FFF, 10 MV and 10 FFF beams and for each beam, charge measured with a PTW Unidos Webline Electrometer. The detector warm up stability was measured with a series of four 6 MV 200 monitor unit (MU) deliveries, with a three hour gap between irradiations. Dose rate dependence was assessed by varying the dose rate from ~50 MU/min, to the maximum achievable dose rate for each energy (400–2150 MU/min). The linearity in response with varying MU (range 5–2000) was measured relative to an IBA CC13 detector. The reproducibility of point dose measurements in a typical clinical plan

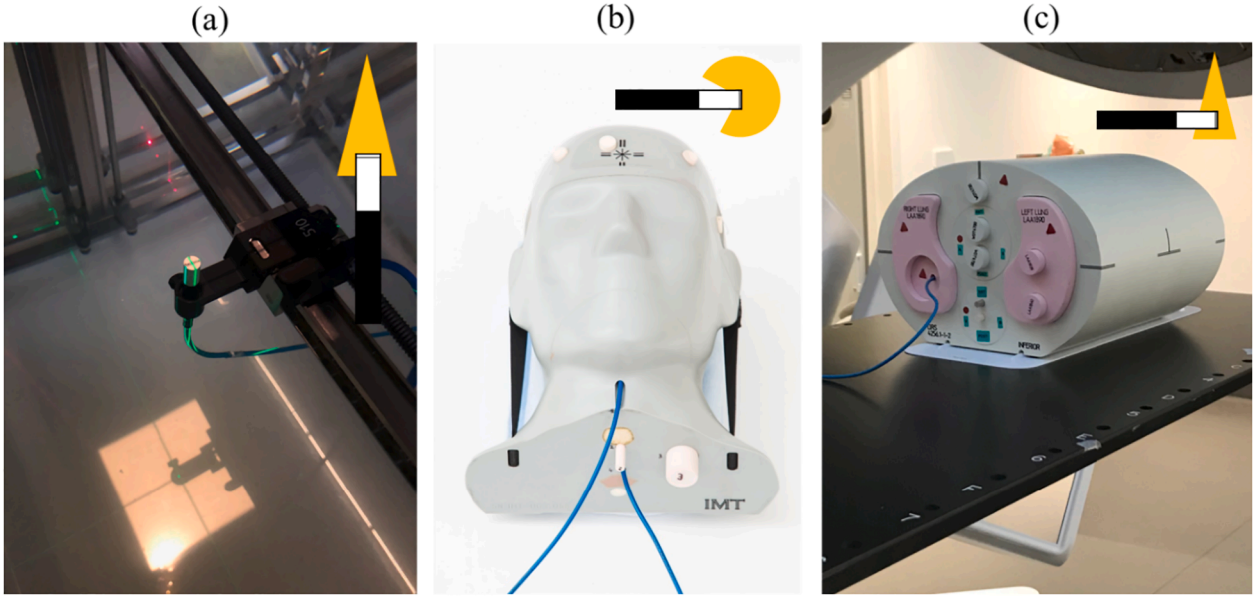

Fig. 1. (a) PTW microDiamond detector in the beam parallel orientation, (b) ACDS cranial phantom with two craniocaudal microDiamond detectors and (c) ACDS thorax phantom with microDiamond detector measurement in lung target. Typical orientations of the beam relative to the detector axis are shown in the schematics.

was established by delivering the same VMAT SBRT plan to the thorax phantom seven times. In the SBRT spine audit case, two microDiamonds were placed in the phantom for concurrent measurements of target dose and spinal cord dose. The effect of detector shadowing from the two microDiamonds aligned in the coronal plane was assessed by delivering a single posterior beam, a VMAT SBRT spine plan and a seven field IMRT SBRT spine plan to the thorax phantom with (a) both detectors in place and (b) with only the target detector and the spinal cord detector cavity plugged with tissue equivalent material.

2.2. Cross-calibration

The seven detectors were cross-calibrated using a normalised dose to water (N_{Dw}) approach [20] against a Farmer type secondary standard ionisation chamber (PTW 30013), traceable to the Australian Primary Standard [21–23]. The detectors were setup under reference conditions in water at 90 cm SSD, 10 cm depth, 10x10 cm^2 field. The microDiamond detectors were orientated parallel to the incident down-facing beam. Cross-calibration factors, N_{Dw,Q_cross}, were determined for 6 MV, 6 FFF, 10 MV and 10 FFF at the respective maximum dose rates (400-2150 MU/min). To assess the uncertainty in the cross-calibration procedure, it was repeated three times for detector sn122179. To assess long term stability, the process was repeated for four individual detectors at 1.8–2.2 years after initial calibration.

For SRS and SBRT dosimetry audits, the microDiamond detectors were placed into the phantoms craniocaudally, and thus perpendicular to the beam axis in co-planar delivery. Hence a correction for the response difference between perpendicular and parallel orientations, $k_{perpendicular}$, was determined. For each of the seven microDiamond detectors, field size and energy specific correction factors were determined for 10 × 10, 3 × 3, 2 × 2 and 1 × 1 cm^2 fields, and 6 MV, 6FFF, 10 MV and 10FFF beam energies. Inplane and cross-plane dose profiles were scanned to determine the centre of each of the radiation fields. $k_{perpendicular}$ was calculated as the ratio of the detector response in parallel to that in the perpendicular orientation.

Four microDiamond detectors were also cross-calibrated on the Gamma Knife system (Elekta AB, Stockholm, Sweden) using an IBA CC04 secondary standard ionisation chamber, traceable to the Australian Primary Standard. The detectors were setup in reference conditions in the Elekta Solid Water reference phantom at 32 cm SSD, 8 cm depth, with all sources out using the 16 mm collimators. In the Gamma Knife setting, the Co-60 sources were orientated in a range of angles relative to the detector axis. The calibration was considered a 'total correction factor', encompassing all angular corrections for the all sources out configuration.

Small field output factors were calculated via secondary analysis of data collected for cross calibration and are shown in Supplementary Fig. S1. Field size dependent corrections from TRS-483 were applied using the irradiated full width half maximum (FWHM) field size corrections [12].

2.3. Angular dependence

Two aspects of angular dependence were considered; coplanar and non-coplanar, defined with respect to the craniocaudally orientated detector. For co-planar delivery, the roll response of the detector was considered with the beam always perpendicular to the detector axis. For non-coplanar delivery, the angular dependence in the pitch and yaw axis was considered. (Supplementary Fig. S2)

To determine the non-coplanar angular dependence of the microDiamond, the detector was compared to an IBA RAZOR (CC01) ionisation chamber, who's response in the parallel vs perpendicular orientation was measured to be within 0.7% for all energies and field sizes. Measurements were performed in a 30 × 30 × 30 cm^3 CIRS plastic water phantom at 85 cm SSD and 15 cm depth, for 6 MV and 6FFF beams with field sizes 3 × 3 cm^2 and 1.5 × 1.5 cm^2. Both detectors were placed craniocaudally into the phantom and their responses compared at gantry and couch angles 0–90° in 30° increments. The non-coplanar experiment was normalised to the detector perpendicular orientation (Gantry 0°, couch 0°) for each energy and field size, to match the audit conditions. Non-coplanar angular dependence correction factors, k_{ncp}, were determined for couch angles in 45° increments, averaging responses from all gantry angles.

Characterisation of the coplanar roll response was performed for three microDiamond detectors, each setup in a water phantom at 90 cm SSD, 10 cm depth, and orientated perpendicular to the down-facing beam. 6 MV, 6FFF, 10 MV and 10FFF beams of 3 × 3 cm^2 field size were delivered to the detector, which was rotated in ~30° increments, as rotating the gantry was not feasible due to the presence of the water tank. The measurement at each position was compared to the average reading from all positions. The coplanar roll response was also characterised in the presence of a magnetic field in two Magnetic Resonance Linear Accelerators (MR-Linac). Measurements were performed on an Elekta Unity with the magnetic field orientated perpendicular to the radiation beam, and the Australian MR-Linac (AML, Ingham Institute, Sydney, Australia) with the magnetic field orientated parallel to the radiation beam. Comparisons were made between the Unity 7 FFF beam, the AML 6 FFF beam and the ARPANSA VersaHD 6 FFF beam with no magnetic field.

2.4. Positional sensitivity in SRS and SBRT

The positional sensitivity of the microDiamond in a small field was determined by irradiating three individual detectors with a 6MV, 1 × 1 cm^2 MLC defined field using the couch to shift the detector in 1 mm increments in the lateral, longitudinal and vertical directions. The microDiamond was placed perpendicular to the beam in a Solid Water phantom at 90 cm SSD, 10 cm depth.

The positional uncertainty in an SBRT plan was determined by shifting 2D dose planes from 6MV VMAT plans for soft tissue, spine and lung SBRT audit cases in silico. The dose planes were shifted ±1 mm in the horizontal and vertical directions. At each shifted position, the matrix was subtracted from the original matrix, and compared for a region of interest at the microDiamond measurement point.

2.5. Overall measurement uncertainty

An overall measurement uncertainty budget was derived for SRS and SBRT deliveries considering the detector properties discussed in Sections 2.1–2.4.

3. Results

3.1. Basic dosimetric properties

The warm up stability was found to be within <0.2% for repeated 200 MU deliveries with extended time intervals between sets of irradiations. A 2 Gy dose was determined to provide sufficient detector warm up, well below the manufacturer recommended 5 Gy. The dose rate dependence was within 0.7% for all energies. The linearity was found to be within 0.5% above 30 MU, relative to a CC13 reference detector for all energies. The standard deviation in detector response from the seven deliveries of the same VMAT SBRT plan was 0.3% (±0.1%). Detector shadowing caused a dose difference of 1.6% for a single posterior field, 0.5% for an IMRT field and 0.1% for a VMAT field.

3.2. Cross-calibration

Large variations were found in the $N_{Dw,\ Q\_cross}$ calibration factors for the seven detectors in parallel orientation (Table 1). Repeatability of the cross calibration procedure was within 0.5% (SD 0.2%) for a single detector. The long term stability of the average calibration factor across

Table 1
PTW 60019 microDiamond cross-calibration factors for 6 MV and Co-60 Gamma Knife.

microDiamond sn	N_{Dw,Q_cross} (6MV) parallel orientation (mGy/nC)	Total calibration factor (Co-60 Gamma Knife) (mGy/nC)
122179	1.017	–
123242	0.777	0.770
123244	0.766	–
123669	1.199	1.201
124007	0.780	0.781
124008	0.935	0.935
124146	0.860	–

all energies was within 0.4% for four detectors.

The calibration factor was established for a range of beam qualities (Co-60 Gamma Knife, and MV beams with $TPR_{20,10}$ 0.684–0.733), with all detectors showing a relatively flat energy response (Fig. 2a). Relative to the 6 MV factor, the largest energy dependence was for 10 MV, with an average of 0.6% difference in the calibration factor (maximum 0.9%).

The average $k_{perpendicular}$ correction factors for the seven detectors ranged from 0.950 to 0.982 (Fig. 2b). For all field sizes except the 1 × 1 cm^2, the $k_{perpendicular}$ factors for the different energies agreed within the standard uncertainty. For the 1 × 1 cm^2 field, the range of $k_{perpendicular}$ factors varied within 1.6%.

3.3. Angular dependence

The angular dependence of the diamond detector relative to the CC01 was up to 3.9% for non-coplanar angles between direct perpendicular and parrallel orientations (Fig. 3). Non-coplanar correction factors, k_{ncp}, were dervied for a range of couch angles from the average response at all gantry angles, as shown in Supplementary Table S1.

For the Conventional Linac measurements, the roll response was within 2% for three detectors at each roll position (Fig. 4a). The average for each position was calculated from all energies, as the difference in readings between energies was less than 0.3% for all three detectors (standard uncertainty within 0.2%). The maximum roll position difference was 1.2%, 1.0% and 1.3% for detectors sn123444, sn123424 and sn123669, respectively. The roll response of detector sn123244 was within 1.4% in a Conventional 6FFF beam and two types of MR-Linacs (Fig. 4b).

3.4. Sensitivity to positioning in a SBRT plan

For the 1 × 1 cm^2 static field, the measured dose was within 1% of the maximum response within ±1 mm in the longitudinal, lateral and vertical directions. When the detector was shifted ± 2 mm away from the maximum response, the difference extended to within ±4% for the longitudinal and lateral shifts, and remained within ±1% for the vertical shifts.

For the VMAT SBRT plan, after shifting the plan ±1 mm in the horizontal and vertical planes, the average difference in the measurement point region was 0.6%, 1.0% and 0.7% for the soft tissue, spine and lung plans respectively.

3.5. Overall uncertainty budget

The overall measurement uncertainty was 3.6% (2σ) for diamond detector point dose measurement in an SRS treatment plan (Table 2). For an SBRT measurement, the non-coplanar angular dependence component is generally not applicable, therefore the overall measurement uncertainty reduces to 3.1% (2σ). The uncertainty due to cross-calibration is shown in Supplementary Table S2.

4. Discussion

Diamond detectors orientated perpendicular to the beam axis enable QA measurements in solid phantoms, and are advantageous in end-to-end testing and PSQA as they provide real time results. Seven diamond detectors were cross-calibrated against secondary standard ionisation chambers, angular corrections presented and an overall uncertainty derived for measurement in SRS and SBRT plans. The overall performance of the seven detectors was very similar, demonstrating the robustness of the detector design/model, and the ability for detectors to be used interchangeably across dosimetry audits.

This study has compared seven individual detectors, the oldest and newest of which have serial numbers ~2000 apart. A large variation in the cross calibration factor was found between individual detectors (N_{Dw,Q_cross} calibration factors, Table 1). This is in contrast to a local cohort of 11 Farmer-type ionisation chambers, which have <1% variation in N_{Dw}. This variation can be attributed to manufacturing differences in the amount of active material of the detector, as discussed by Butler et al. [24]. The long term stability of the cross-calibration factor showed that cross-calibration should occur every 2–3 years, in line with TRS-398 recommendations [20].

The majority of SRS treatments are delivered including non-coplanar

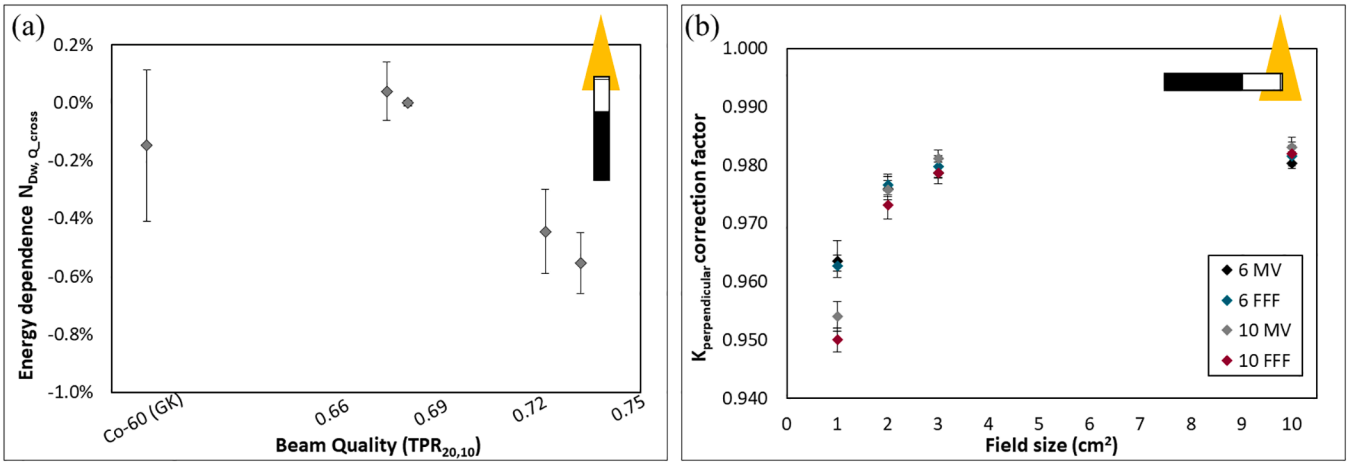

Fig. 2. (a) Average energy dependence, relative to 6MV, of N_{Dw,Q_cross} calibration factors for seven PTW 60019 microDiamond detectors in the beam parallel orientation. The error bars show standard uncertainty from calibration of seven detectors. (b) Average parallel vs perpendicular correction factors ($k_{perpendicular}$) for nominal beam field size at detector EPOM and nominal beam energies, for the seven detectors. The error bars show the standard uncertainty.

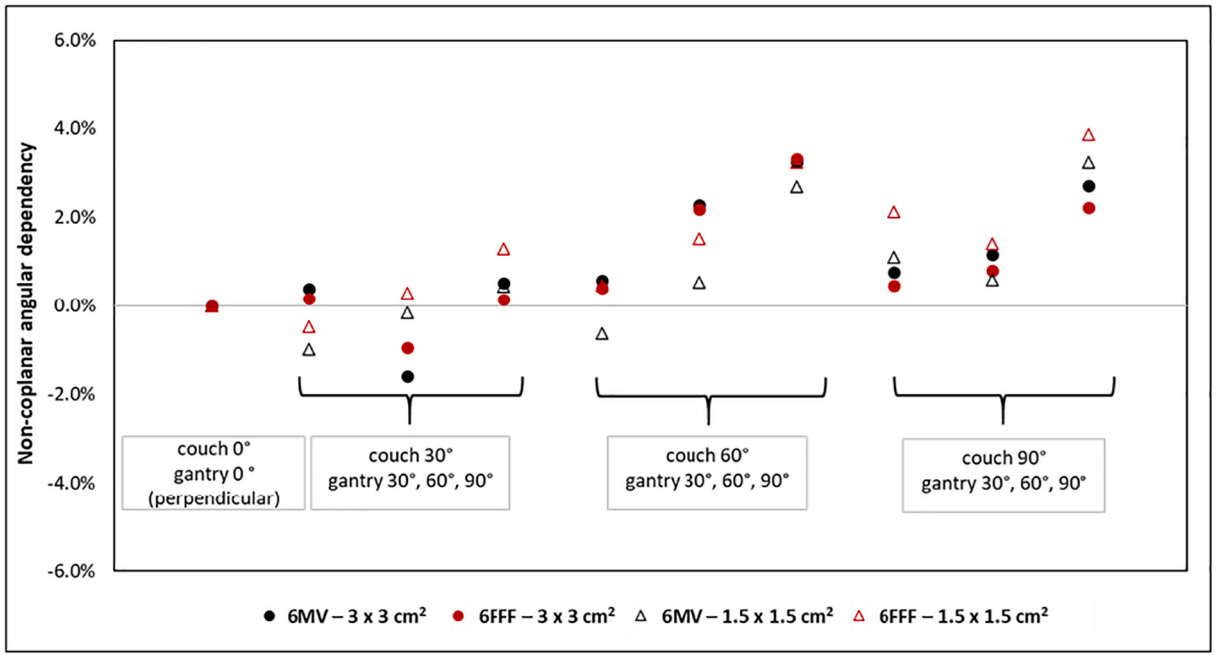

Fig. 3. Non-coplanar angular dependence of microDiamond for 6 MV and 6 FFF with 3 × 3 cm^2 and 1.5 × 1.5 cm^2 fields, compared to RAZOR chamber. In each grouping of couch angle, the data series shown left to right represent the gantry angles of 30°, 60°, and 90° respectively.

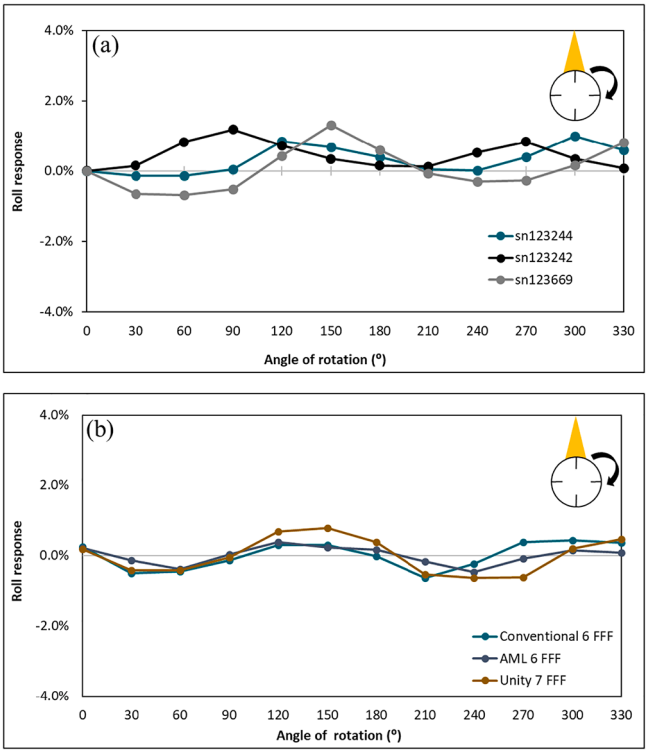

Fig. 4. (a) Roll response of three microDiamond detectors measured with 6 MV, 6 FFF, 10 MV and 10 FFF on a VersaHD Linac. The roll response at each position is relative to the average response of all positions. (b) Roll response of microDiamond sn123244 in Conventional 6 FFF Linac, and inline and perpendicular MR-Linac configurations.

beams/arcs with rotation of the couch and gantry in Conventional Linear Accelerators, or with inherent non-coplanar delivery such as the Gamma Knife or Cyberknife. The non-coplanar angular dependence of the diamond detector was found to be within 5% for a range of clinically deliverable gantry and couch angles. These results agree with studies performed by Brace et al. [18] and Veselsky et al. [25] who found similar angular dependencies for gantry angles up to 70°, but very large angular dependencies of up to 30% when irradiating through the stem of the detector. These beam angles would not be clinically deliverable in SRS treatment plans delivered on a conventional linac, and have therefore not been considered by in this study. In SRS audit deliveries, it is difficult to determine the specific gantry and couch angle combinations in treatment plans, and therefore tailor the required correction factors, as

Table 2
Overall point dose measurement in SRS/SBRT treatment plan uncertainty budget.

Quantity	Relative standard uncertainty	
	100 u_{iA}[1]	100 u_{iB}[2]
Phantom/detector positioning uncertainty	–	0.8
k_T	–	0.0
k_P	–	0.0
k_H	–	0.0
Electrometer calibration factor	–	0.15
$N_{Dw,\ Q\_cross}$ calibration factor	–	0.73
Non-coplanar angular dependence	–	0.9
Coplanar roll response	–	0.3
Linearity	–	0.5
Dose rate	–	0.7
k_s (recombination)	–	0.0
k_{pol} (polarity)	–	0.0
k_n (beam non uniformity)	–	0.0
(field output correction factor)	–	0.4
Reproducibility of SABR delivery and detector charge measurements	0.3	–
Facility daily output	–	0.4
Quadratic summation	**0.3**	**1.78**
Combined relative standard uncertainty (k = 1)	**1.80**	

[1] u_{iA} represents the relative standard uncertainty estimated by statistical methods, type A.
$2u_{iB}$ represents the relative standard uncertainty estimated by other means, type B.

the delivery parameters vary widely from centre to centre. For audit purposes, the k_{ncp} correction factor for the 45° couch angle was taken as the nominal 'average' for all plans and is applied to measurement of the whole plan. Application of couch angle specific correction factors would be achievable in individual centres with controlled planning parameters.

The roll response varied up to 1.3% for single beam irradiation. This could have significant impact on the measurement of single beams (including for PSQA normalisation), or when 'collapsing' all beams to gantry 0° for PSQA. Roll response is not likely to have significant impact for VMAT cases where it would average out. To minimise its impact, each detector was marked at the average roll response and used in this orientation for cross-calibration. No significant difference was found in the roll response due to the presence of a magnetic field, in agreement with the results of Woodings et al. [26].

The overall measurement uncertainty of 3.6% and 3.1% (2σ) for SRS and SBRT treatment deliveries respectively, considers the measurement only and does not take into account uncertainties from the treatment plan. Due to the presence of steep dose gradients, careful consideration of the planned dose distribution should be made when making point dose comparisons in SRS and SBRT verification measurements.

In conclusion, this study showed that synthetic diamond detectors were reliable and robust detectors for end-to-end dosimetry in SRS and SBRT applications. Such detectors allow accurate real time point dose measurements during PSQA and end-to-end testing, and pair well with spatial dosimetry offered by 2D detectors. The orientation of the detector relative to the beam axis is an important consideration, as significant corrections are required for angular dependence.

Declaration of Competing Interest

The authors declare that they have no known competing financial interests or personal relationships that could have appeared to influence the work reported in this paper.

Acknowledgements

The authors would like to thank the following centres for contributions to the research; the Townsville Cancer Centre, the Ingham Institute for Applied Medical Research (Australian MRI Linac) and the Peter MacCallum Cancer Centre.

This research is supported by an Australian Government Research Training Program (RTP) Scholarship.

Appendix A. Supplementary data

Supplementary data to this article can be found online at https://doi.org/10.1016/j.phro.2021.10.002.

References

[1] Distefano G, Baker A, Scott AJD, Webster GJ. Survey of stereotactic ablative body radiotherapy in the UK by the QA group on behalf of the UK SABR Consortium. Br J Radiol 2014;87:20130681.
[2] Pan H, Simpson DR, Mell LK, Mundt AJ, Lawson JD. A survey of stereotactic body radiotherapy use in the United States. Cancer 2011;117:4566–72.
[3] Nagata Y, Hiraoka M, Mizowaki T, Narita Y, Matsuo Y, Norihisa Y, et al. Survey of stereotactic body radiation therapy in Japan by the Japan 3-D Conformal External Beam Radiotherapy Group. Int J Radiat Oncol Biol Phys 2009;75:343–7.
[4] Foote M, Bailey M, Smith L, Siva S, Hegi-Johnson F, Seeley A, et al. Guidelines for safe practice of stereotactic body (ablative) radiation therapy. J Med Imaging Radiat Oncol 2015;59:646–53.
[5] Kirkbride P, Cooper T. Stereotactic body radiotherapy. Guidelines for commissioners, providers and clinicians: a national report. WB Saunders 2011;23:163–4.
[6] Sahgal A, Roberge D, Schellenberg D, Purdie T, Swaminath A, Pantarotto J, et al. The Canadian Association of Radiation Oncology scope of practice guidelines for lung, liver and spine stereotactic body radiotherapy. Clin Oncol 2012;24:629–39.
[7] SABR UK Consortium. A stereotactic ablative body radiation therapy (SABR): A resource. The Faculty of Clinical Oncology of the Royal College of Radiologists 2019;v6.1.
[8] Halvorsen PH, Cirino E, Das IJ, Garrett JA, Yang J, Yin FF, et al. AAPM-RSS medical physics practice guideline for SRS-SBRT. J Appl Clin Med Phys 2017;18:10–21.
[9] Bruschi A, Esposito M, Pini S, Ghirelli A, Zatelli G, Russo S. How the detector resolution affects the clinical significance of SBRT pre-treatment quality assurance results. Phys Med 2018;49:129–34.
[10] Clark CH, Hurkmans CW, Kry SF, on behalf of The Global Quality Assurance of Radiation Therapy Clinial Trials Harmonisation Group. The role of dosimetry audit in lung SBRT multi-centre clinical trials. Phys Med 2017;44:171–6.
[11] Wen N, Lu S, Kim J, Qin Y, Huang Y, Zhao B, et al. Precise film dosimetry for stereotactic radiosurgery and stereotactic body radiotherapy quality assurance using Gafchromic™ EBT3 films. Radiat Oncol 2016;11:132.
[12] IAEA Technical Report Series No. 483. Dosimetry of small static fields used in external beam radiotherapy: An International Code of Practice for reference and relative dose determination. Sponsored by IAEA and AAPM. 2017.
[13] Kairn T, Charles PH, Cranmer-Sargison G, Crowe SB, Langton CM, Thwaites DI, et al. Clinical use of diodes and micro-chambers to obtain accurate small field output factor measurements. Australas Phys Eng Sci Med 2015;38:357–67.
[14] Russo S, Masi L, Francescon P, Frassanito MC, Fumagalli ML, Marinelli M, et al. Multicenter evaluation of a synthetic single-crystal diamond detector for CyberKnife small field size output factors. Phys Med 2016;32:575–81.
[15] Ralston A, Tyler M, Liu P, McKenzie D, Suchowerska N. Over-response of synthetic microDiamond detectors in small radiation fields. Phys Med Biol 2014;59:5873–81.
[16] De Coste V, Francescon P, Marinelli M, Masi L, Paganini L, Pimpinella M, et al. Is the PTW 60019 microDiamond a suitable candidate for small field reference dosimetry? Phys Med Biol 2017;62:7036–55.
[17] Lárraga-Gutiérrez JM, Ballesteros-Zebadúa P, Rodríguez-Ponce M, García-Garduño OA, de la Cruz OOG. Properties of a commercial PTW-60019 synthetic diamond detector for the dosimetry of small radiotherapy beams. Phys Med Biol 2015;60:905–24.
[18] Brace OJ, Alhujaili SF, Paino JR, Butler DJ, Wilkinson D, Oborn BM, et al. Evaluation of the PTW microDiamond in edge-on orientation for dosimetry in small fields. J Appl Clin Med Phys 2020;21:278–88.
[19] Williams I, Kenny J, Lye J, Lehmann J, Dunn L, Kron T. The Australian Clinical Dosimetry Service: a commentary on the first 18 months. Australas Phys Eng Sci Med 2012;35:407–11.
[20] IAEA Technical Report Series No. 398. Absorbed dose determination in external beam radiotherapy: an international code of practice for dosimetry based on standards of absorbed dose to water. IAEA. 2000, v12.
[21] Wright T, Lye JE, Ramanathan G, Harty PD, Oliver C, Webb DV, et al. Direct calibration in megavoltage photon beams using Monte Carlo conversion factor: validation and clinical implications. Phys Med Biol 2015;60:883–904.
[22] Butler DJ, Ramanathan G, Oliver C, Cole A, Lye J, Harty PD, et al. Direct megavoltage photon calibration service in Australia. Australas Phys Eng Sci Med 2014;37:753–61.
[23] Ramanathan G, Harty P, Wright T, Lye J, Butler D, Webb D, et al. The Australian Primary Standard for absorbed dose to water (graphite calorimeter). 2014.
[24] Butler DJ, Beveridge T, Lehmann J, Oliver CP, Stevenson AW, Livingstone J. Spatial response of synthetic microDiamond and diode detectors measured with kilovoltage synchrotron radiation. Med Phys 2018;45:943–52.
[25] Veselsky T, Novotny Jr J, Pastykova V. Assessment of basic physical and dosimetric parameters of synthetic single-crystal diamond detector and its use in Leksell Gamma Knife and CyberKnife small radiosurgical fields. Int J Radiat Res 2018;16:7–16.
[26] Woodings SJ, Wolthaus JWH, van Asselen B, de Vries JHW, Kok JGM, Lagendijk JJW, et al. Performance of a PTW 60019 microDiamond detector in a 1.5 T MRI-linac. Phys Med Biol 2018;63:05NT04.